Power law for frequency-dependence of double layer capacitance of graphene flakes

Power law for frequency-dependence of double layer capacitance of graphene flakes

Hongxin Wang, Koichi Jeremiah Aoki, Jingyuan Chen*, Toyohiko Nishiumi, Xiangdong Zeng, Xiuyuan Ma

Department of Applied Physics, University of Fukui, 3-9-1 Bunkyo, Fukui 910-0017, Japan

ARTICLE INFO

Article history:
Received 22 October 2014
Received in revised form 7 January 2015
Accepted 10 January 2015
Available online xxxx

Keywords:
Double layer capacitance of graphene films
Frequency-dispersion
Constant phase element
Density of graphene

ABSTRACT

The double layer capacitance per weight of graphene (GN) flakes in aqueous solution at the polarized potential increases with a decrease in the ac-frequency, obeying the inverse of the power law of the frequency. The power law is demonstrated to be equivalent to the constant phase element. The frequency-dependence increases with the thickness of the GN films. Thus, the lower the frequency and the thinner the film is, the larger is the capacitance density per weight. This is confirmed by cyclic voltammetry for several thickness of GN films and several scan rates. Resistance-like voltammograms at thick films are caused by frequency -dispersion. The overall capacitive properties of the GN films are as follows: the thickness of one GN flake is estimated to be 2 nm in average from the comparison of the thickness with the capacitances at the HOPG, which is consistent with values by the STM and AFM images.

1. Introduction

Carbon powder has been used as stacked electrode materials, which include carbon nanotubes, carbon nano fibers, and graphene powder. These materials have been explored for candidates of supercapacitors. Thicker carbon films obviously enhance the capacitance. They also increase frequency-dependence of their capacitors [1,2], because the dependence is generally exhibited more strongly at electrodes with surface roughness of fractal dimension [3–10], with high porosity [11–13], heterogeneous distributions of current density [14–17], inhomogeneous adsorption [18], and inhomogeneous coating materials [19,20]. The common reason for the frequency dependence is heterogeneity of electrodes. Since the capacitance varies with both thickness and frequency complicatedly, it is not easy to predict capacitance values *a priori*. It is of interest to find a general rule of governing them in the context of thickness and frequency. First of all, we discuss the general behavior of the frequency dependence in the light of the impedance measurements.

The frequency dependence has been interpreted as distribution of various time constants of double layer capacitors [21]. A traditional equivalent circuit for the double layer impedance is an ideal capacitor, which is connected in series with the solution resistance [22]. The circuit in series should yield a vertical line in a Nyquist plot [23,24], whereas the Nyquist plots of real double layer capacitances have frequently provided lines with slopes less than 10 [25]. The non-vertical line has been modeled by the so-called constant phase element (CPE) [26–30]. The impedance of the CPE, Z_{CPE}, is expressed by the power α, ranging from 0 to 1, of a complex impedance. i.e.

$$Z_{CPE} = 1/(Q(i\omega)^{\alpha}) = \{\cos(\pi\alpha/2) - i\,\sin(\pi\alpha/2)\}/(Q\omega^{\alpha}) \quad (1)$$

where ω is angular velocity of applied ac-voltage, and Q is a constant. The slope of the line in the Nyquist plot is $\tan(\pi\alpha/2)$. The CPE can reproduce experimental results well, but does not explain any origin of physicochemical phenomena such as frequency-dispersion and adsorption [31]. The data analysis by the CPE is close to the analysis with a frequency-independent phase angle different from 90° [28].

We have explained Eq. (1) as an inevitable result of the frequency-dispersion [25,32–34], as follows. The time-derivative of the double layer charge q, i.e. $I = dq/dt$, at the capacitance, C, for the applied voltage $V = V_o \exp(i\omega t)$ is given by

$$I = \frac{d(C(\omega)V(t))}{dt} = C(\omega)\frac{dV(t)}{dt} + V(t)\frac{dC(t)}{dt} \quad (2)$$

Values of dC/dt are not conventionally available, but those of $dC/d\omega$ are readily available. Since $\omega = t^{-1}$, we have

$$\frac{dC(t)}{dt} = \frac{dC}{d(1/t)}\frac{d(1/t)}{dt} = -t^{-2}\frac{dC}{d\omega} \quad (3)$$

Consequently, Eq. (2) can be rewritten as

$$I = i\omega CV - t^{-2}V\frac{dC}{d\omega} = \left(i\omega C - \omega^2\frac{dC}{d\omega}\right)V \quad (4)$$

The admittance in Eq. (4), $i\omega CV - \omega^2(dC/d\omega)$, is the sum of the out-of-phase component and the in-phase component. Hence the equivalent circuit can be expressed in terms of a parallel combination of C (defined as C_p) and the resistance ($-\omega^{-2}/(dC/d\omega) = R_p$). The parallel combination of the double layer has been introduced by Bockris et al. [35] in order to explain dielectric relaxation. It has been verified experimentally by changing solution resistance [25] as well as fitting experimental results [19]. The parallel resistance R_p, depending on frequency, has been demonstrated to have surface properties in that it does not only vary with distance between two electrodes [32], with salt concentrations [33], or kinds of solvents [25], but also it is inversely proportional to the area of electrode surfaces [33]. The double layer capacitance, C_d, conventionally observed can be then expressed as

$$i\omega C_d = 1/R_p + i\omega C_p \tag{5}$$

This is nothing but the admittance ($1/Z$) of the conventionally observed double layer impedance, Z. The relations between Eqs. (1) and (5) are

$$|Q\omega^{\alpha}| = \sqrt{R_p^{-2} + \omega^2 C_p^2} = \omega\sqrt{(f(dC_p/df))^2 + C_p^2} \tag{6}$$

$$\tan(\pi\alpha/2) = \omega C_p R_p = -C_p/\{f(dC_p/df)\} \tag{7}$$

where R_p was replaced on the right-hand sides by $-\omega^{-2}/(dC/d\omega)$. Since C_p has a linear relation with $\log f$ [25,32,33], the term $(dC_p/df)f$ is almost constant. Then α can be determined unequivocally through Eq. (7). The correspondence of the CPE to the frequency-dependence in Eqs. (6) and (7) indicates that the CPE behavior should result quantitatively from the frequency-dispersion.

The above quantitative interpretation of the CPE does not elucidate a physical meaning of the frequency-dispersion. It is not easy to evaluate domain size of heterogeneity although few attempts have been reported on local electrochemical impedance spectroscopy [36–38]. Since the frequency-dependence at highly oriented pyrolytic graphite (HOPG) electrode is less than that at polycrystalline platinum electrodes [32,39], the domain size of heterogeneity may be of the order of magnitude of roughness or grain of polycrystalline surface.

When conducting powder-like materials are accumulated on an electrode as in supercapacitors, the heterogeneity may increase to enlarge the CPE effect, or to decrease α. Since the capacitance is given by $Q/\omega^{1-\alpha}$ from Eq. (1), the enlarged CPE effect decreases the capacitance values with an increase in the frequency. Consequently, values of the capacitances should be specified by not only values of α but also the frequency or the time to be used for measurements. This report aims at finding an empirical rule of dependence of the capacitances made of graphene (GN) flakes on frequency and GN thickness.

2. Experimental

Water was distilled and then was ion-exchanged by a ultrapure water system, CPW-100 (Advantec, Tokyo). All the chemicals were of analytical grade. Graphite powder (98%, 7 μm in average diameter) was purchased from Ito Koken (Mie, Japan), and was used as received. HOPG was purchased from Bruker Corp. Before each voltammetric run and coating processes for the electrodes, the HOPG surface was exfoliated with adhesive tape.

The suspension of graphite oxide (GO) was prepared according to the Hummers method [40]. Removal of salt from the suspension was made by centrifugation a cooling centrifuge (Tomy, Tokyo) at the maximum, 10,600g and by dispersion in pure water. The centrifugation and the dispersion were iterated three times. An aliquot of the purified suspension was dried and weighed to determine the weight concentration. A GO suspension of 100 mm^3 with a known concentration was dropped on the exfoliated HOPG plate (12×12 mm^2), and was dried in an oven at 60 °C for one hour. The dried GO film was reduced chemically with 0.2 M (=mol dm^{-3}) hydrazine monohydrate aqueous solution in a vessel kept at 90 °C for one hour [41] to yield the GN film. The reduced film was rinsed with water. Two GO- and two GN-coated HOPG plates were prepared simultaneously. They were faced each other with the space of ca 5 mm, supported a rubber block. 0.5 M KCl solution was filled into the space, as shown in Fig. 1(A).

Density of the dried GN, ρ, was determined by means of pycnometry, which was used for evaluating the density of swollen polyacrylic latex particles [42]. The method was to obtain weights of a ca 50 cm^3 dried pycnometer (m_0) and that (m_w) of the pycnometer into which water was filled. The difference divided by the density of water, $\rho_w = 0.997$ g cm^{-3}, is the volume of the pycnometer at 25 °C. The suspension of GN, which was deionized by centrifugation, was filled in the pycnometer, and weighed (m_s). The pycnometer filled with the suspension was dried at 90 °C in an oven for one day, was cooled to the room temperature, and weighted (m_{sd}). Then the volume of the pycnometer can be represented by the two ways:

$$V = \frac{m_w - m_0}{\rho_w} = \frac{m_s - m_{sd}}{\rho_w} + \frac{m_{sd} - m_0}{\rho} \tag{8}$$

Then ρ is given by

$$\frac{\rho}{\rho_w} = \frac{m_{sd} - m_0}{m_w - m_0 - m_s + m_{sd}} \tag{9}$$

The four weights were obtained reproducible with the digit of mg. Then we had $\rho = 1.29 \pm 0.01$ g cm^{-3}. We applied the above method to the GO suspension to evaluate the density of dried GO. It was 1.26 ± 0.03 g cm^{-3}. Both densities are almost the same within errors. According to the thermogravimetry previously made [43], the GN flakes contain graphite oxide inside.

A drop of 0.5 M KCl solution was inserted into two GO- or GN-coated plates. The contact area of the KCl drop was evaluated from photographs, on the basis of which Fig. 1(A) was drawn. The difference in the shape of the menisci for the GO and GN supports higher hydrophobicity of GN than GO. The thickness of the film was calculated from the added volume of the GO suspension with the known weight concentration, the area of the electrode in contact with the solution, and the densities.

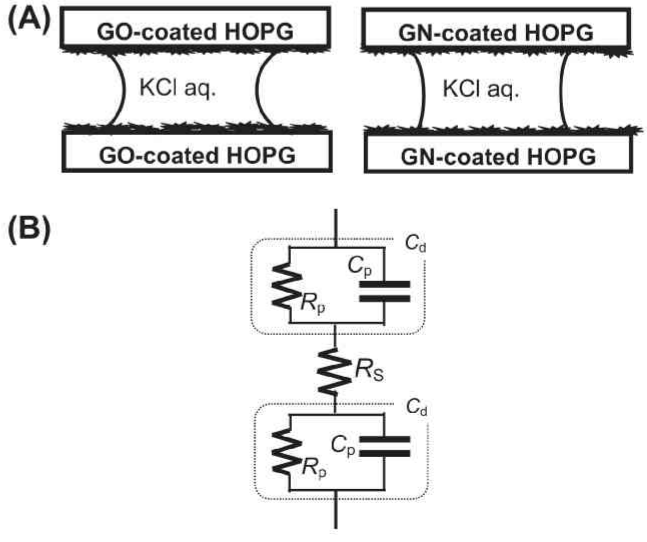

Fig. 1. Cell structure for ac-impedance measurements (A), and its equivalent circuit (B).

Ac-impedance was obtained in the symmetric cell in Fig. 1(A) with a potentiostat, Compactstat (Ivium Tech., Netherlands). The equivalent circuit is a series connection of the two conventionally observed double layer capacitances, C_d, and the solution resistance, R_s. The applied ac-voltage was 10 mV in amplitude with the frequency ranging from 0.1 Hz to 3 kHz. Cyclic voltammetry was made in this symmetric cell.

Scanning tunneling microscope (STM) was NanoScope (MSE-FFAC001, Veeco). STM images were taken in air in a dry room. Atomic force microscope (AFM) was Nanocute (Hitachi).

3. Results and discussion

We prepared GN- and GO-films with various thicknesses on the HOPG. The thickness, which was evaluated from the volume of the suspension with the known weight concentration and the density of GN or GO, is an average value over the electrode. Since the density was evaluated from the volume of water excluding the volume of GN or GO without considering dead space among GN (GO) particles, the geometrical thickness of the film is larger than the calculated one.

The surface of the GO-coated HOPG showed vague STM images even at any magnification except for extremely thin films. The vagueness may be ascribed partly to less electrical conductivity of the GO, and partly to very rough surface of GO that cannot be layered. In contrast, GN-coated HOPG exhibited STM images which included a flat plane and a lump with stripes, as shown in Fig. 2(A). Since the magnification of the flat plane showed honeycomb structure of crystalline HOPG, the plane should be a bare HOPG surface. The lump has crystalline structure with many stripes, which may stand for layered surfaces of GN flakes. Fig. 2(B) shows a height profile of the line in Fig. 2(A). The height of the lump is not uniform

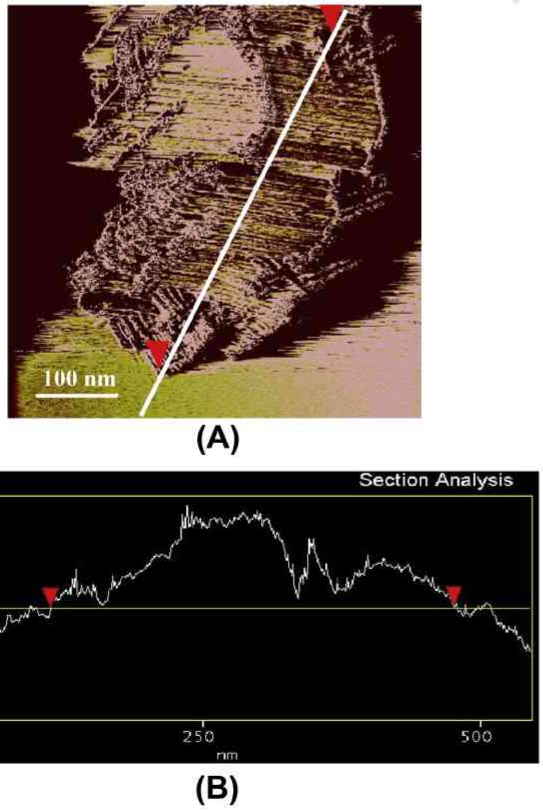

Fig. 2. STM image (A) of the GN-coated HOPG with 1.1 nm thickness and the height profile (B) on the line in (A).

probably because the exfoliation by Hummers' method occur at incontrollable layers of graphite. It was the thinnest film (1.4 nm) that exhibited the geometry-defined images such as Fig. 2(A).

Since the maximum view window of the STM, $(0.5\ \mu m)^2$, cannot cover the whole size of a GN flake, we used AFM to see the geometry and the surface of a flake. Fig. 3 shows the AFM image, which includes a flake with $1 \times 2\ \mu m^2$. The height profile shows the thickness of the flake with a few nanometers.

Ac-impedance of the films was obtained in 0.5 M KCl aqueous solution by the two-electrode cell (Fig. 1(A)) at 10 mV ac amplitude. The dc-potential of the impedance data is a rest potential. Fig. 4 shows Nyquist plots at the GN- and the GO-coated HOPG. The plots for the GO films with 0.011 μm (a) were overlapped with those of the GN films (not shown because of the overlap). Both of them were almost the same as the Nyquist plot at the HOPG (the line). Therefore, the GO and GN have no influence on the impedance data so far as thickness was less than 0.011 μm. The slope of the line was ca 8.5, corresponding to $\alpha = 0.93$. Thick GN films decreased values of $-Z_2$ more than those of Z_1, yielding the decrease in the slope. In contrast, the Nyquist plots for GO did not vary with the thickness (c). This is because GO is an electric insulator.

Since the present measurement is made at two identically coated substrate electrodes (HOPG), the total impedance is a series combination of the solution resistance, R_s, and two parallel combinations of C_p and R_p, as is shown in Fig. 1(B), where both C_p and R_p are frequency-dependent, satisfying $1/(\partial C/\partial t) = R_p$. This equivalent circuit can be represented by

$$Z_1 + iZ_2 = R_s + \frac{2}{1/R_p + i\omega C_p} \tag{10}$$

The explicit forms of C_p and R_p can be solved to be given by

$$C_p = \frac{-Z_2}{\omega}\frac{1}{(Z_1 - R_s)^2 + Z_2^2}, \quad R_p = \frac{(Z_1 - R_s)^2 + Z_2^2}{2(Z_1 - R_s)} \tag{11}$$

We determined the solution resistance, R_s, by extrapolating the Nyquist plots to the Z_1 axis. The R_s values ranged from 30 to 80 Ω, depending on the distance between two substrate electrodes. Since they had no relation with the film thickness, they do not contain the resistance of the film. Values of C_p and R_p were determined from Z_1 and Z_2 at each frequency through Eq. (11).

We found previously that C_p at platinum electrodes had a linear relation with logarithmic frequency with a negative slope [25,32–34]. We plotted C_p values for the HOPG, the GO- and the GN-coated electrodes against log$f$, and obtained also the linear relation except for thick GN films. The logarithmic linearity is only an empirical relationship without any theoretical background, and hence other types of relationship are possible, for example, a power relation given by

$$C_p = (C_p)_{f=1} f^{-\lambda} \tag{12}$$

for positive values of λ, where $(C_p)_{f=1}$ is the value of C_p at 1 Hz. The plot of log(C_p) against log$f$ for HOPG exhibited a line with the coefficient of determination over 0.994. The linearity in C_p vs. log$f$ for small variation of C_p is approximated by the linearity in log(C_p) vs. log$f$, as can be seen from the Taylor expansion, $\ln(a + x) = \log a + x/a + \ldots$ for small values of x. Fig. 5 shows plots of logC_p against log$f$ for the GO- and the GN-coated HOPG with two kinds of the thickness. Most of the plots fell on each line, although slight deviation was found at high frequency. The deviation was smaller than that of the plot of C_p vs. log$f$. All the values of C_p for the GN films were larger than those of the GO. This fact indicates that GN should provide large surface area in contact with the solution. Values of C_p for GN increase with an increase in the film thickness.

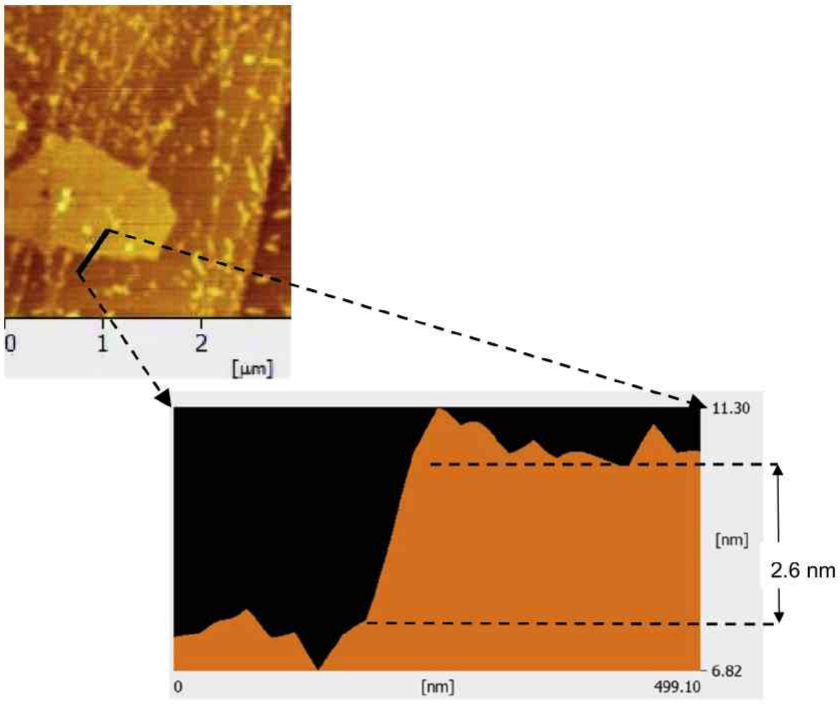

Fig. 3. AFM image of the GN-coated HOPG with 1.1 nm thickness and the height profile near the step.

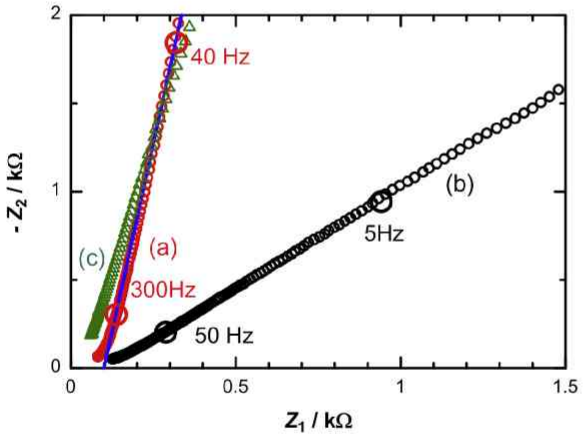

Fig. 4. Nyquist plots of the GN films with thickness (a) 0.011 μm, (b) 1.1 μm and (c) GO film with 1.1 μm in 0.5 M KCl aqueous solution in the frequency domain from 1.4 to 2500 Hz. The solid lines are the Nyquist plots at the HOPG electrode.

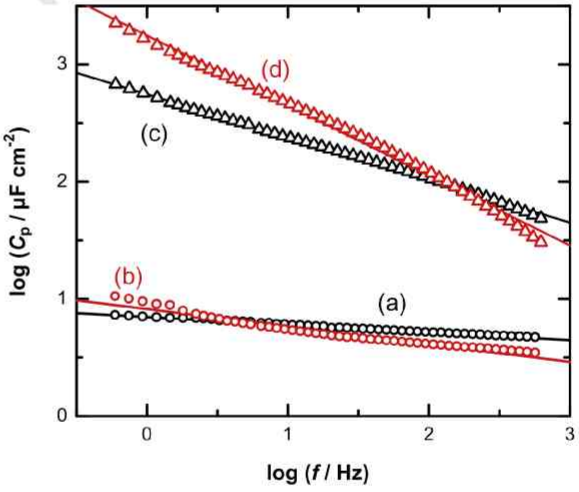

Fig. 5. Logarithmic variations of C_p with the frequency at (a, b) GO-coated HOPG and (c, d) GN-coated HOPG for the film thickness of (a, c) 0.077 μm and (b, d) 1.1 μm.

In order to examine the variation of C_p with the film thickness, we firstly pay attention to $(C_p)_{f=1}$. Fig. 6 shows the variations of $(C_p)_{f=1}$ of GO and GN with the film thickness, δ. The values of $(C_p)_{f=1}$ for GO did not vary with δ. The average value was 4 ± 2 μF cm^{-2}, which is not far from the value (7.5 μF cm^{-2} from Fig. 3) for the bare HOPG. The similarity suggests no contribution of GO to an increase in the electroactive surface area, because GO is an electrical insulator which covers partially the active area of HOPG. In contrast, the values of $(C_p)_{f=1}$ of GN increase largely with an increase in the thickness. Especially, they are proportional to the thickness for $\delta < 0.11$ μm, as shown in the inset of Fig. 6. The proportionality has been found by the stacking layer-by-layer technique of graphene [38]. It indicates that each graphene flake should exhibit the capacitive property common to all the layers. The slope of the proportionality is 8.3 μF cm^{-2} nm^{-1}. We assume that the capacitance per one surface of a GN flake is the same as that of HOPG (7.5 μF cm^{-2}). A GN flake has two surfaces; being a fore plane and a back plane. Then the capacitance of a GN flake per cm^2 is 15 μF. Consequently, one flake ought to have the thickness 1.8 (=15/8.3) nm per HOPG plane in average. This value is smaller than the thickness observed by the AFM images in Fig. 3, partly because the capacitance includes surface roughness on GN flakes (in STM), and partly because the observed AFM images were for flakes thick enough of getting clear observation.

Fig. 7 shows the variation of λ (the power in Eq. (12)) with the logarithms of the film thickness. Values of λ both for GO and GN at $\delta < 10$ nm are close to the value of λ for HOPG (horizontal line). On the other hands, those for GN at $\delta > 10$ nm enhance linearly with $\log\delta$, i.e., $\lambda = 0.24 \log(\delta/\text{nm}) + 0.62$. Since λ is a measure of the frequency-dependence, the increase in λ implies a rise of the dependence by the thickness. When combining the relation with $(C_p)_{f=1} = 8.3\ (\delta/\text{nm})$ μF cm^{-2} for the proportional domain in Fig. 6, we can rewrite Eq. (12) as

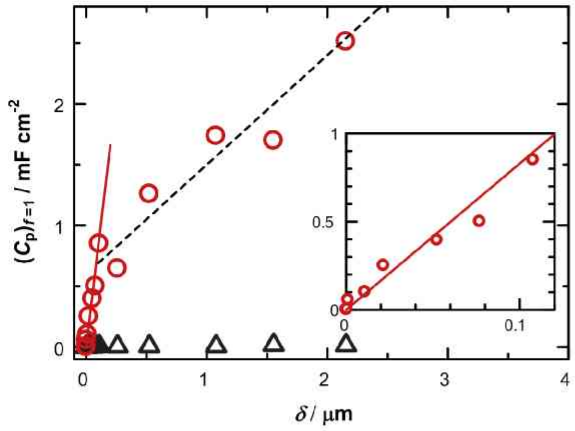

Fig. 6. Dependence of C_p at $f = 1$ for (triangles) GO- and (circles) GN-coated HOPG electrodes on the thickness of the films, δ. The inset is the magnification of C_p for thin GN films.

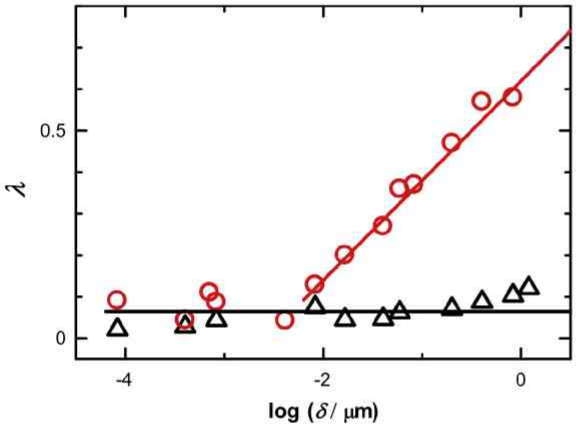

Fig. 7. Variations of λ for (triangles) GO and (circles) GN with logarithm of the film thickness. The horizontal line is for HOPG.

$$C_p = 8.3\delta f^{-0.24\ \log\delta + 0.11}\ \mu\text{F cm}^{-2}, \tag{13}$$

where the unit of δ is nm. Inserting this equation into Eq. (7) yields

$$\tan(\pi\alpha/2) = 1/\lambda = 1/(0.24\log\delta - 0.11) \tag{14}$$

It implies that the slope of the line in the Nyquist plot should decrease with an increase in the thickness. Since Eq. (13) includes δ in the power, the capacitance is not accurately proportional to δ or the number of the GN layers, n. Letting the capacitance with n layers be C_{pn}, values of C_{pn} may be smaller than the n times of the capacitance with one-layer, i.e. nC_{p1}, with an increase in frequency. According to Eq. (13), nC_{p1}, is expressed by

$$C_{pn} = nC_{p1}f^{-0.24\ \log n} \tag{15}$$

Fig. 8 shows variations of the ratio, C_{pn}/nC_{p1}, with log f, calculated from Eq. (15) for several values of n. With an increase in the thickness (n), the capacitance is less than nC_{p1}. This inequality is larger at higher frequency.

Values of super-capacitors have often been obtained by means of chronopotentiometry, chronoamperometry and cyclic voltammetry (CV) rather than ac impedance methods. It is of interest to examine how the frequency-dependence may be realized in current- or voltage–time curves. Here we restrict our discussion to CV. Voltammetry was made at the cell of Fig. 1 in the polarized potential domain. Fig. 9 shows voltammograms at two GN films with different thickness. The voltammograms at the thin film (A)

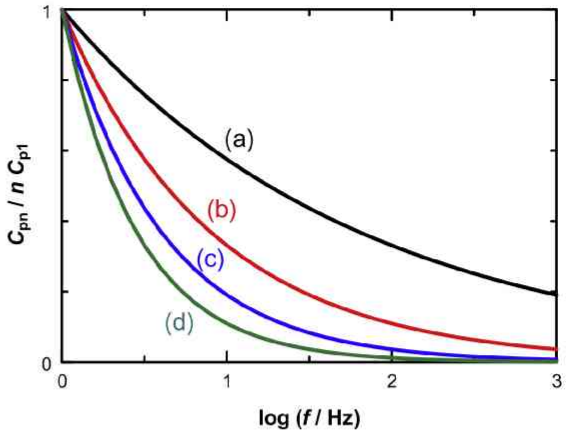

Fig. 8. The frequency-dependence of the capacitance with n-layered thick films for n = (a) 10, (b) 100, (c) 1000, and (d) 10,000, calculated from Eq. (13).

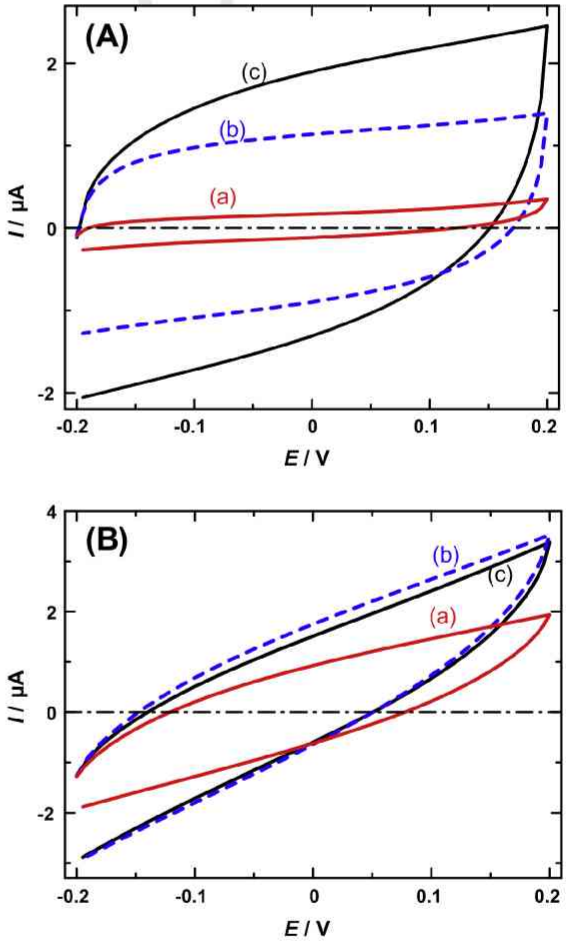

Fig. 9. Cyclic voltammograms at the GN-coated HOPG electrode coated with the GN films (A) 0.077 μm and (B) 2.2 μm in thickness in 0.5 M KCl solution at ν = (a) 10, (b) 50 and (c) 100 mV s^{-1}.

take a conventional shape of background voltammograms, i.e. being similar to a parallelogram. In contrast, those at thick film (B) deformed from a conventional one as if they include a large ohmic-like contribution. Since both cells have values of R_s as low as 40 Ω by the impedance measurement, the solution resistance should have no effect on the voltammetric shape. A possible reason for the deformation is a participation in the parallel resistance, R_p.

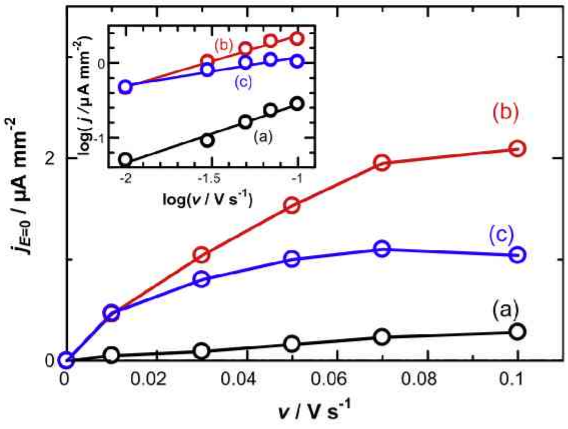

Fig. 10. Plots of the voltammetric current density at $E = 0.0$ V against scan rates at the films for δ = (a) 0.077, (b) 0.53 and (c) 1.1 μm, obtained in 0.5 M KCl solution. The inset is the plot on the logarithmic scales.

Fig. 10 shows plots of the anodic and the cathodic currents at $E = 0.0$ V in Fig. 9 against the scan rates, v, for different thicknesses of the GN films. Although capacitive currents at a bare electrode are generally proportional to v, the variation in Fig. 10 shows that the currents have v^{β}-dependence for $0 < \beta < 1$, e.g. $\beta = 0.78$, 0.69 and 0.37 for $\delta = 0.077$, 0.53 and 1.1 μm, respectively, as shown in the inset of Fig. 10. The scan rate dependence is equivalent to the inverse of the time-dependence. Inserting Eq. (13) into Eq. (2) and applying this equivalence to Eq. (2) yields approximately

$$I = C_p \frac{dE}{dt} + E\frac{dC_p}{dt} = C_p v + kE\, t^{0.24\log\delta - 1.11} \approx kV^{-0.24\log\delta + 1.11} \qquad (16)$$

Then, values of the power, $-0.24\log(\delta) + 1.11$, are 0.65, 0.46 and 0.38 for the above values of δ, respectively. These values are close to those β, determined in Fig. 10. The difference is due to the difference in the voltammetry time scale from that of the ac-impedance. It is the frequency-dispersion that causes the deformation of voltammograms for thick films.

4. Conclusions

The frequency-dispersion can be represented quantitatively as $f^{-\lambda}$ by use of the positive value, λ. Then the CPE parameter α is related with λ through Eq. (14). Consequently, the slope of a line in Nyquist plots, is given by $-Z_2/(Z_1 - R_s) = \tan(\pi\alpha/2) = 1/\lambda$. The parameter α or λ not only expresses the frequency-dispersion but also confirm the presence of R_p.

The frequency-dispersion at GN-coated and the GO-coated HOPG electrodes are obeyed by the power law. The GO-coating does not influence the capacitance because GO is an electric insulator. In contrast, the GN-coating enhances the capacitance, which is almost proportional to the thickness of the layer. The comparison of the thickness and the capacitances yields 2 nm thickness of one GN flake in average.

The frequency-dispersion per given thickness increases with the thickness. Thus, the lower the frequency and the thinner the film is, the larger is the capacitance density. The time-dependence of the capacitance requires us to specify the frequency or the time of the capacitance measurements when capacitance values are reported. The frequency-dispersion is reflected even on deformation of cyclic voltammograms from a parallelogram to a line of an ohmic resistance when films get thick. Then the voltammetric currents are not proportional to v but is obeyed by the power law, v^{β}. Q3

Acknowledgment

This work was financially supported by Grants-in-Aid for Scientific Research (Grant 25420920) from the Ministry of Education in Japan.

References

[1] G. Láng, K.E. Heusler, J. Electroanal. Chem. 377 (1994) 1.
[2] T. Pajkossy, J. Electroanal. Chem. 364 (1994) 111.
[3] L. Nyikos, T. Pajkossy, Electrochim. Acta 30 (1985) 1533.
[4] Z. Kerner, T. Pajkossy, Electrochim. Acta 46 (2000) 207.
[5] J.B. Bates, Y.T. Chu, W.T. Stribling, Phys. Rev. Lett. 60 (1988) 627.
[6] U. Rammelt, G. Reinhard, Electrochim. Acta 35 (1990) 1045.
[7] E.D. Bidoia, L.O.S. Bulhoes, R.C. Rocha-Filho, Electrochim. Acta 39 (1994) 763.
[8] R. de Levie, Electrochim. Acta 10 (1965) 113.
[9] B. Sapoval, R. Gutfraind, P. Meakin, M. Keddam, H. Takenouti, Phys. Rev. E 48 (1993) 3333.
[10] T. Pajkossy, Hetero. Chem. Rev. 2 (1995) 143.
[11] A. Lasia, J. Electroanal. Chem. 397 (1995) 27.
[12] C. Hitz, A. Lasia, J. Electroanal. Chem. 500 (2001) 213.
[13] H.-K. Song, H.-Y. Hwang, K.-H. Lee, L.H. Dao, Electrochim. Acta 45 (2000) 2257.
[14] R.D. Armstrong, W.P. Race, J. Electroanal. Chem. 34 (1972) 244.
[15] H.H. Bauer, M.S. Spritzer, P.J. Elving, J. Electroanal. Chem. 17 (1968) 299.
[16] M.E. Orazem, P. Agarwal, L.H. Garcia-Rubio, J. Electroanal. Chem. 378 (1994) 51.
[17] M. Durbha, M.E. Orazem, B. Tribollet, J. Electrochem. Soc. 146 (1999) 2199.
[18] T. Pajkossy, T. Wandlowski, D.M. Kolb, J. Electroanal. Chem. 414 (1996) 209.
[19] J.-B. Jorcin, M.E. Orazem, N. Pebere, B. Tribollet, Electrochim. Acta 51 (2006) 1473.
[20] C.A. Schiller, W. Strunz, Electrochim. Acta 46 (2001) 3619.
[21] J.R. MacDonald, Trans. Faraday Soc. 66 (1970) 943.
[22] M. Sluyters-Rehbach, Pure Appl. Chem. 66 (1994) 11831.
[23] A.J. Motheo, J.R. Santos Jr., A. Sadkowski, A. Hamelin, J. Electroanal. Chem. 397 (1995) 331.
[24] A.J. Motheo, A. Sadkowski, R.S. Neves, J. Electroanal. Chem. 430 (1997) 253.
[25] Y. Hou, K.J. Aoki, J. Chen, T. Nishiumi, J. Phys. Chem. C 118 (2014) 10153.
[26] J.R. Macdonald (Ed.), Impedance Spectroscopy, Wiley, New York, 1987.
[27] A. Lasia, in: R.E. White, B.E. Conway, J.O'M. Bockris (Eds.), Modern Aspects of Electrochemistry, vol. 32, Kluwer Academic/Plenum Publishers, New York, 1999, p. 143.
[28] G.J. Brug, A.L.G. Van Den Eeden, M. Sluyters-Rehbach, J.H. Sluyters, J. Electroanal. Chem. 176 (1984) 275.
[29] P. Zoltowski, J. Electroanal. Chem. 443 (1998) 149.
[30] J.R. Macdonald, J. Phys. Chem. C 117 (2013) 23433.
[31] M.H. Martin, A. Lasia, Electrochim. Acta 56 (2011) 8058.
[32] K. Aoki, Y. Hou, J. Chen, T. Nishiumi, J. Electroanal. Chem. 689 (2013) 124.
[33] Y. Hou, K.J. Aoki, J. Chen, T. Nishiumi, Univ. J. Chem. 1 (2013) 162.
[34] X. Zhao, K.J. Aoki, J. Chen, T. Nishiumi, RSC Advances 4 (2014) 63171–63181.
[35] J.O'M. Bockris, E. Gileadi, K. Mueller, J. Chem. Phys. 44 (1966) 1445.
[36] E. Bayet, F. Huet, M. Keddam, K. Ogle, H. Takenouti, Electrochim. Acta 44 (1999) 4117.
[37] G. Baril, C. Blanc, M. Keddam, N. Pebere, J. Electrochem. Soc. 150 (2003) B488.
[38] Z. Lei, T. Mitsui, H. Nakafuji, M. Itagaki, W. Sugimoto, J. Phys. Chem. C 118 (2014) 6624.
[39] K.J. Aoki, H. Wang, J. Chen, T. Nishiumi, Electrochim. Acta 130 (2014) 381.
[40] W.S. Hummers, R.E. Offeman, J. Am. Chem. Soc. 80 (1958) 1339.
[41] C. Vallés, P. Jiménez, E. Muñoz, A.M. Benito, W.K. Maser, J. Phys. Chem. C 115 (2011) 10468.
[42] T. Li, K. Aoki, J. Chen, T. Nishiumi, J. Electroanal. Chem. 656 (2011) 279.
[43] J. Chen, X. Zeng, K.J. Aoki, T. Nishiumi, Langmuir, 2014 (submitted for publication). Q4